Stem Cell Research & Therapy

RESEARCH

Open Access

DVL/GSK3/ISL1 pathway signaling: unraveling the mechanism of SIRT3 in neurogenesis and AD therapy

Nan Dai[1†], Xiaorong Su[2†], Aihua Li[1], Jinglan Li[3], Deqi Jiang[4] and Yong Wang[1,5*]

Abstract

Background The established association between Alzheimer's disease (AD) and compromised neural regeneration is well-documented. In addition to the mitigation of apoptosis in neural stem cells (NSCs), the induction of neurogenesis has been proposed as a promising therapeutic strategy for AD. Our previous research has demonstrated the effective inhibition of NSC injury induced by microglial activation through the repression of oxidative stress and mitochondrial dysfunction by Sirtuin 3 (SIRT3). Nonetheless, the precise role of SIRT3 in neurogenesis remains incompletely understood.

Methods In vivo, SIRT3 overexpression adenovirus was firstly injected by brain stereotaxic localization to affect the hippocampal SIRT3 expression in APP/PS1 mice, and then behavioral experiments were performed to investigate the cognitive improvement of SIRT3 in APP/PS1 mice, as well as neurogenic changes in hippocampal region by immunohistochemistry and immunofluorescence. In vitro, under the transwell co-culture condition of microglia and neural stem cells, the mechanism of SIRT3 improving neurogenesis of neural stem cells through DVL/GSK3/ISL1 axis was investigated by immunoblotting, immunofluorescence and other experimental methods.

Results Our findings indicate that the overexpression of SIRT3 in APP/PS1 mice led to enhanced cognitive function and increased neurogenesis. Additionally, SIRT3 was observed to promote the differentiation of NSCs into neurons during retinoic acid (RA)-induced NSC differentiation in vitro, suggesting a potential role in neurogenesis. Furthermore, we observed the activation of the Wnt/ß-catenin signaling pathway during this process, with Glycogen Synthase Kinase-3a (GSK3a) primarily governing NSC proliferation and GSK3ß predominantly regulating NSC differentiation. Moreover, the outcomes of our study demonstrate that SIRT3 exerts a protective effect against microglia-induced apoptosis in neural stem cells through its interaction with DVLs.

Conclusions Our results show that SIRT3 overexpressing APP/PS1 mice have improved cognition and neurogenesis, as well as improved neurogenesis of NSC in microglia and NSC transwell co-culture conditions through the DVL/GSK3/ISL1 axis.

Keywords SIRT3, Neural stem cells, Neurogenesis, Neuronal differentiation, Wnt/β-catenin pathway

[†]Nan Dai and Xiaorong Su have contributed equally to this study

*Correspondence:
Yong Wang
wy43555@smu.edu.cn
Full list of author information is available at the end of the article

Introduction

Alzheimer's disease (AD) is a progressive neurodegenerative disorder characterized by a decline in memory and cognitive functions among patients [1]. There is a widespread consensus that the observed cognitive decline in both AD patients and experimental animal models is primarily attributable to the impairment of neural network integrity [2]. Moreover, the depletion of basal forebrain cholinergic neurons and synapses in the brains of AD patients leads to circuit dysfunction, exacerbating the manifestations of the disease. AD is further characterized by a deterioration of cognitive abilities, frequently accompanied by neuropsychiatric symptoms such as anxiety-like behaviors [3]. Comprehending the underlying mechanisms of these cognitive and non-cognitive symptoms is paramount for devising comprehensive therapeutic strategies and addressing other neuropsychiatric manifestations. While traditional approaches to ameliorating cognitive decline in AD have focused on preserving neuronal viability, these treatments have proven less effective than anticipated [4, 5]. Consequently, fostering neurogenesis has emerged as a viable strategy to mitigate cognitive decline and its associated symptoms, including anxiety. Neurogenesis, an intricate process encompassing the proliferation, differentiation, migration, maturation, and functional integration of neural stem cells (NSCs) [6], presents a promising avenue for revealing novel therapeutic targets and advancing the treatment of AD.

Sirtuin3 (SIRT3), a NAD+-dependent deacetylase, is closely associated with cell development and has garnered significant attention in recent years for its role in neurodegenerative diseases, including AD [7–10]. Notably, the neuroprotective effect of PACAP was abolished upon SIRT3 knockdown using shRNA in primary cultured neurons, highlighting its importance in neuronal health [11]. SIRT3 has also been demonstrated to mitigate mitochondrial dysfunction and neuronal damage by impeding mito-p53 function [12]. Additionally, SIRT3 promotes the development of aged NSCs through its physical interaction with long-chain acyl-CoA dehydrogenase (LCAD), further underscoring its potential therapeutic value [13]. Our previous study indicated that SIRT3 can ameliorate NSC damage induced by microglial activation through the mitochondrial apoptosis pathway, suggesting a mechanism by which SIRT3 may contribute to the maintenance of neural integrity and, consequently, the alleviation of AD symptoms, including anxiety [14]. However, the precise molecular mechanism by which SIRT3 influences NSC development and its role in modulating anxiety in AD remains elusive and warrants further investigation.

LIM homeodomain (LIM-HD) transcription factor Islet-1 (ISL-1) is expressed in cholinergic neurons of the spinal cord, hindbrain, forebrain, and retina. Deletion of ISL-1 results in the loss of cholinergic neurons in the spinal cord and hindbrain [15]. Furthermore, conditional deletion of ISL-1 using Six3-Cre transgenic mice leads to a reduction of cholinergic neurons in the forebrain and retina [15]. These findings collectively underscore the role of ISL-1 in determining cholinergic neuronal fate in the central nervous system of vertebrates [16]. Therefore, this study will observe the expression of ChAT and ISL-1 to determine the differentiation of cholinergic neurons in each group.

Initially characterized as a pivotal regulator of tumorigenesis, the Wnt/β-catenin signaling pathway is now widely recognized as an essential modulator of homeostasis in developmental and adult NSCs [17, 18]. It has become apparent that Wnt/β-catenin signaling is intricately involved in adult neurogenesis [19–21], being activated during the differentiation of neural stem/progenitor cells [22–24]. Mazemondet et al. underscored the significance of spatio-temporal modulation of the Wnt/β-catenin pathway during human neural progenitor cell differentiation [25]. Given the crucial role of the Wnt/β-catenin pathway in NSC proliferation and differentiation, we hypothesized that SIRT3 promotes neurogenesis through Wnt/β-catenin signaling.

Methods

Animals and treatments

All animal experiments were approved by the Ethics Committee of Zhujiang Hospital, Southern Medical University, and conducted in accordance with the ARRIVE guidelines. Twelve male APP/PS1 transgenic mice (weighing 30–40 g, aged 6 months) and six age- and sex-matched wild-type (WT) mice (not littermates but from the same strain, weighing 30–40 g, aged 6 months) were obtained from the Animal Experimental Center of Zhujiang Hospital, Southern Medical University. After purchasing the mice, they were allowed to acclimatize to the environment for one month, meaning experiments would commence when the mice reached 7 months of age. The mice were housed in an environment where humidity and temperature could be controlled, with free access to food and water, and experienced a 12-h light/dark cycle each day.

To minimize pain and suffering before and after surgery, we implemented a strict pain management procedure. Prior to surgery, we anesthetized the mice using tribromoethanol (0.2 ml/10 g, intraperitoneally) to ensure that they were unconscious and did not feel pain during the procedure. During surgery, we insisted on the use of aseptic techniques to minimize infection and associated pain. After surgery, we place the mice in a warm and quiet recovery area and monitor post-surgical pain

by regularly checking their behavior and appearance. We are prepared to use analgesics for pain relief if needed.

To examine the effects of SIRT3 on neurogenesis in APP/PS1 mice, the APP/PS1 and WT mice were assigned to the following three groups based on their genotype (n = 6 mice per group): WT group, APP/PS1 group, and APP/PS1 + SIRT3 group. As shown in Fig. 1A, the mice were allowed to acclimate for 4 weeks prior to the experiment and subsequently received intracerebral injections of AAV. Following the injections, the mice underwent a recovery period of 4 weeks before behavioral tests were conducted. Subsequently, a further 4-week interval was observed before immunohistochemistry and immunofluorescence experiments were performed.

Open field test (OFT)

The anxiety-like behavior of the mice was evaluated using the open field test (OFT), a widely accepted method for assessing anxiety in rodents, including those with transgenic AD models. The experimental apparatus, constructed from 50 cm × 50 cm × 50 cm white high-density, non-porous plastic, featured a 25 cm × 25 cm central zone. Prior to the commencement of the experiment, the mice were allowed to acclimate to the testing environment for 3 h. Subsequently, the mice were placed in the central area and allowed to explore freely for 5 min. The EthoVision XT 15 software was utilized to record the total distance traveled and the duration spent in the central area during the experiment. Following each trial, the experimental apparatus was cleaned with 75% alcohol.

Morris water maze test (MWM)

The spatial memory and navigational abilities of the mice were assessed through a water maze experiment, with tracking and analysis of the water maze video conducted using EthoVision XT 15 software. The water reservoir was partitioned into four equal quadrants, with a platform randomly positioned at the center of one quadrant, and titanium dioxide added to the water for visibility. The experimental protocol comprised a 5-day training phase followed by a 1-day exploration session. Initially, the platform was placed above the water surface on the first day, and subsequently elevated 1 cm above the water level for the next 4 days. Throughout the training phase, mice were introduced into the water from different quadrant edges in a random sequence each day, and allowed to explore freely for 90 s until they located the platform. In instances where the mice failed to locate the platform within 90 s, they were gently guided to it and allowed to remain there for 10 s. During the exploration session, the platform was removed, and a 90-s trial was conducted to observe the mice's swimming trajectory, residence time in the target quadrant, and the frequency of platform crossings.

Intracerebral injection

SIRT3 was inserted into adeno-associated virus (AAV) vectors obtained from Genepharma, China. The AAV solution was transduced via injection into the lateral ventricles of mice utilizing a brain stereotaxic apparatus from RWD. Mice were anesthetized using isoflurane gas (2.0–2.5%), shaved and then fixed in a stereotaxic frame. Anesthesia was consistently maintained with isoflurane throughout the entirety of the procedure. The bregma served as the reference for the origin of the cranial 3D coordinate system, and bilateral cranial perforations (AP: − 2 mm, LAT: − 1.5 mm, DV: + 1.75 mm) were created with a sterile 0.6 mm drill bit in accordance with the brain stereotaxic atlas. A microinjection system from RWD was employed to deliver 2 ul of AAV (viral titer = 2.49×10^{13} VG/ml) into the bilateral lateral ventricles of the mice at a rate of 100 nl/min. At each coordinate, the needle descended at a rate of 0.32 mm/s and remained stationary for 10 min. Thirty days post-injection, the brains underwent perfusion with 0.9% saline followed by fixation with 4% paraformaldehyde (PFA).

Immunohistochemical studies

Following behavioral assessment, the animals were anesthetized and underwent transcardial perfusion with 0.9% saline. Subsequently, the brains were swiftly excised and fixed in 4% paraformaldehyde for 24 h at 4 °C. Following gradual dehydration in alcohol, the tissue impregnated with wax was embedded using an embedding machine. The paraffin block was then sectioned serially at a thickness of 4 μm using a microtome, and the resulting transverse sections were subjected to hematoxylin and eosin (H&E) (Beyotime, China) as well as Nissl staining (Solarbio, China) according to the manufacturer's guidelines. Assessment of neuronal damage involved quantifying the surviving neuron count in the hippocampal regions of cornu ammonis (CA), CA3, and dentate gyrus (DG) utilizing a microscope from Nikon, Tokyo, Japan. Quantitative analysis was performed on six random fields within each section using Image-Pro Plus software.

Immunofluorescent staining

Coronal sections that were selected underwent overnight incubation at 4 °C with anti-Aβ (1:200, CST, USA), anti-DCX (1:200, CST, USA), and anti-SIRT3 (1:200, CST, USA). Subsequently, an appropriate secondary antibody was applied to the cells and left for 2 h at room temperature. The following secondary antibodies were utilized: goat anti-rabbit IgG (1:400, SeraCare, USA) and goat anti-rat IgG (1:400, SeraCare, USA). DAPI was used

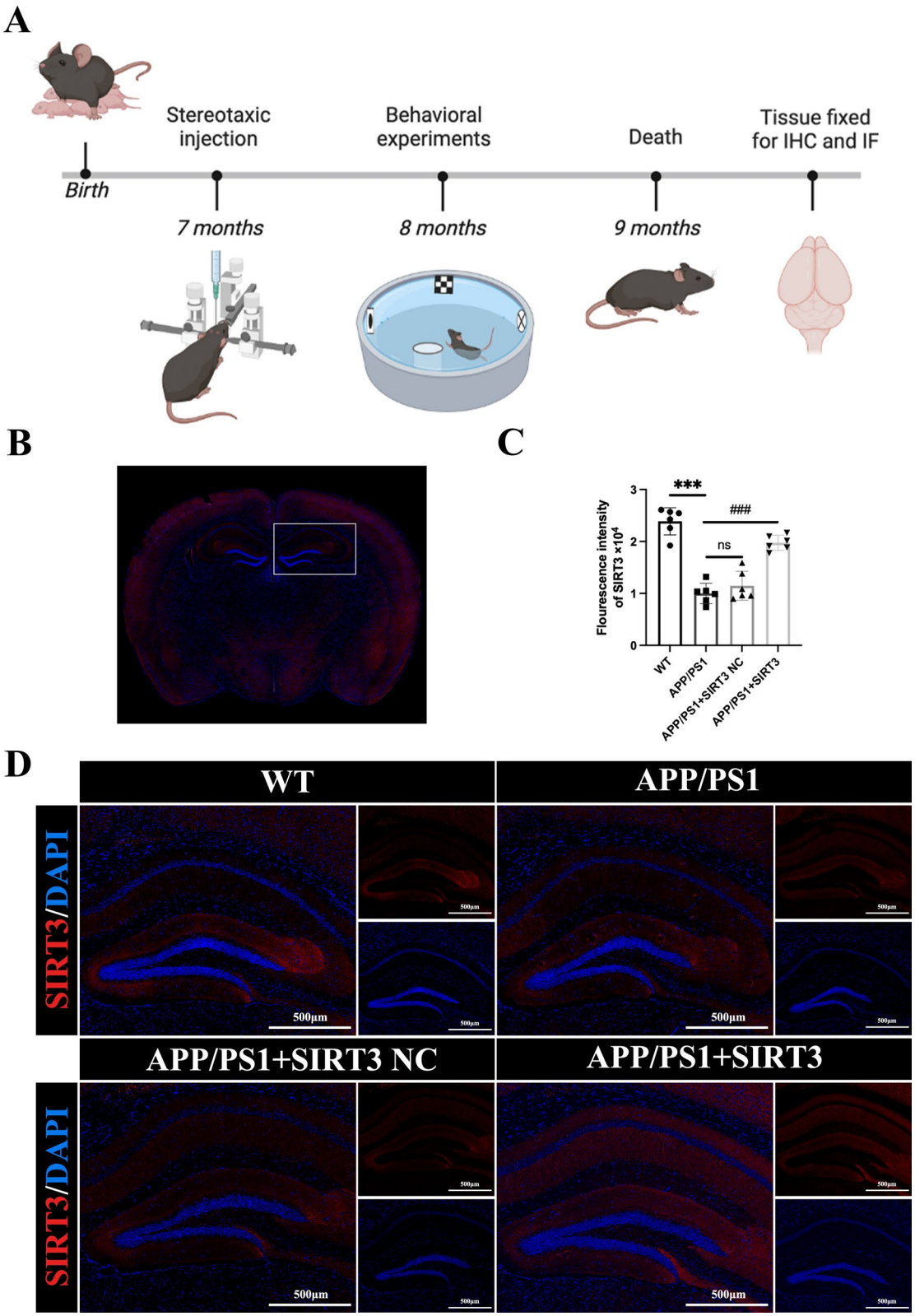

Fig. 1 Decreased SIRT3 expression in APP/PS1 mice. **A** Chronological depiction of in vivo experimentation. **B**–**D** Alterations in SIRT3 expression levels. Scale bar: 500 μm. n = 6; ***P < 0.005; ###P < 0.005

to stain the cell nuclei. Imaging was conducted using a fluorescence microscope from Olympus, Tokyo, Japan. ImageJ software was employed to outline the fluorescence field and to quantify the fluorescence intensity.

Cell lines and cultures

Mouse Neural stem cells (C17.2 cells) were cultured in high-glucose Dulbecco's modified Eagle's medium (DMEM) (GIBCO, Gaithersburg, MD, USA) supplemented with 10% fetal bovine serum (FBS) (Hyclone, Logan, UT, USA), 5% horse serum (Hyclone, Logan, UT, USA), and 1% penicillin/streptomycin (PS) (Invitrogen, Carlsbad, CA, USA). Similarly, mouse microglia (BV2 cells) were maintained in DMEM supplemented with 10% FBS and 1% PS. Cells were incubated at 37 °C with 5% CO2 in a humidified incubator to support their growth.

Cell co-culture

The BV2 cells were cultivated in the upper chambers, while the C17.2 cells were seeded into the lower chambers of a 6-well transwell culture plate, thereby creating a separation between the two cell types using a polycarbonate membrane (0.4 μm pore size; Corning, USA). Aβ peptide was introduced to the microglia at a final concentration of 10 μM. The transwell membrane facilitated the passage of cytokines secreted by the cells, while preventing the free migration of the cells themselves. Following a 48-h co-culturing period of BV2 and C17.2 cells, the C17.2 cells were harvested for experimentation.

Differentiation of NSCs

C17.2 cells in logarithmic phase were induced with 10uM RA (Sigma Aldrich, USA) for 12, 24, 48, 72 and 96 h. The cells were then collected for subsequent experiments.

CCK-8 assay

The CCK-8 kit (GLPBIO, Montclair, CA, USA) was utilized to assess cell proliferation. NSCs were transfected with the specified plasmids or siRNA, and co-cultured with microglia in 6-well plates for 48 h. Subsequently, NSCs were harvested and seeded into 96-well plates at a density of 1×10^5 cells per well. Following this, 100μL of CCK8 incubation solution was added to each well and incubated for 1–4 h, after which the absorbance value at 450 nm was measured using a multifunctional microplate reader (Biotek, USA).

EdU assay

The Cell-lightTM EdU apollo567 in vitro kit (RiboBio, Guangzhou, China) was employed for assessing the proliferation of NSCs. NSCs were isolated from the co-culture system and seeded into 96-well plates. Subsequently, the cells were exposed to EdU (50 μM) labeling media. Following a 2-h incubation period, the NSCs were fixed with 4% paraformaldehyde for 30 min, and then treated with the Apollo reaction cocktail for an additional 30 min. Nuclei were stained using Hoechst 33342. The cells were imaged and quantified using a Nikon Eclipse Ti2 microscopy (Nikon, Tokyo, Japan).

Immunocytochemistry

Immunocytochemistry was conducted on C17.2 cells following slide fixation (4% paraformaldehyde, 15 min). Subsequently, the cells were permeabilized with 0.1% Triton X-100 and blocked with 3% bovine serum albumin (BSA) (Dako, Germany) for 10 min. The cells were then incubated overnight at 4℃ with the following primary antibodies: anti-GFAP (1:1000, Servicebio, GB11096), anti-Tuj1 (1:500, Bioss, bsm-33177 M), anti-Nestin (1:200, ABclonal, A11861). Cell nuclei were counterstained with DAPI, and fluorescence microscopy was used to capture images.

Western blotting

Total proteins were extracted from C17.2 cells using RIPA lysis buffer (Beyotime, China), and their concentrations were determined with the BCA Protein Assay Kit (Bioworld Technology, Co., Ltd, Nanjing, China). Each sample was loaded with 30 μg of total protein and separated on a 10% SDS–polyacrylamide gel, followed by transfer onto a polyvinylidene difluoride membrane (Bio-Rad). Subsequently, the membranes were blocked with 5% nonfat milk or BSA for 1 h and incubated overnight at 4℃ with specific primary antibodies. After that, secondary antibodies were applied and incubated for 1 h at room temperature. The protein signals were visualized using the Uvitec Alliance system (Uvitec, UK). The primary antibodies used in this study including anti-SIRT3 antibody (1:1000, Cell Signaling), anti-GSK3α antibody (1:1000, Cell Signaling), anti-GSK3β antibody (1:1000, Cell Signaling), anti-p-GSK3α antibody (1:1000, Cell Signaling), anti-p-GSK3β antibody (1:1000, Cell Signaling), anti-β-catenin antibody (1:1000, Cell Signaling), anti-p-β-catenin antibody (1:1000, Cell Signaling), anti-Dvl2 antibody (1:1000, Cell Signaling), anti-Dvl3 antibody (1:1000, Cell Signaling), anti-Axin antibody (1:1000, Cell Signaling), anti-Nestin antibody, anti-Tuj1 antibody (1:1000, Abcam), anti-GFAP antibody (1:1500, Servicebio), anti-NeuN antibody (1:1000, Abcam), anti-MAP-2 antibody (1:1000, Abcam), anti-ISL-1 antibody (1:1000, Abcam), anti-GAPDH antibody (1:5000, Proteintech), and anti-HSP90 antibody (1:2000, Proteintech).

Real-time PCR analysis

Gene expression was analyzed through quantitative PCR. Total RNAs were extracted using TRIzol reagent (Ecotop Scientific, China) and quantified with a NanoDrop Spectrophotometer (NanoDrop Technologies, USA). Reverse transcription was carried out using a Color Reverse Transcription Kit (EZBioscience, China). Real-time quantitative PCR reactions were conducted with an ABI Quant Studio3 (Applied Biosystems, US) using the 2×SYBR Green qPCR Master Mix (EZBioscience, China). GAPDH was utilized as the internal control. Primers used were as follows: GSK3α, forward 5′-GGT AGGATGTTTGGGAGATGAG, reverse 5′-ACCACG GCCACACATAAA; GSK3β, forward 5′-GCTGTGTTG GCTGAATTGT, reverse 5′-CTGCTCCTGGTGAGT CCTTT; GAPDH, forward 5′-CATGTTCCAGTATGA CTCCACT, reverse 5′-GTAGACTCCACGACATAC TCAG; Nestin, forward 5′-GGAGAGTCGCTTAGA GGTG, reverse 5′-TCAGGAAAGCCAAGAGAAGC; NeuN, forward 5′-GGGTTTTGGGTTTGTAACTAA CTTTTGAA, reverse 5′-AGACTGCTCCTACCACAG GGTTTAG; MAP-2 forward 5′-AAGGCCAAGAAC ACACGATTG, reverse 5′-GTGTCAGATCGTCCTTAT TC; GFAP forward 5′-AACAACCTGGCTGCGTATAG, reverse 5′-CTGCAAACTTAGACCGATACC.

Flow cytometry

For the assessment of cell apoptosis, the FITC Annexin V and PI Apoptosis Kit (KeyGEN BioTECH, China) was employed following the manufacturer's instructions. C17.2 cells were gathered and incubated with binding buffer, subsequently stained with fluorochrome-conjugated Annexin V-FITC and propidium iodide. The fluorescence imaging was analyzed using a flow cytometer (Beckman Coulter, USA).

Transfection of cells

The full-length GSK3α (NM_001031667) was synthesized and cloned into the expression vector pc-DNA3.1 (Fenghui Biology Co., Ltd, China). Similarly, the full-length GSK3β (NM_019827) was synthesized and cloned into the expression vector pc-DNA3.1-3xFlag-C (Fenghui Biology Co., Ltd, China). GSK3α, GSK3β, Dvl-1, Dvl-2, and Dvl-3 siRNAs were synthesized by GenePharma (China), with all siRNA sequences detailed in Additional file 1: Table S1. Lipofectamine 3000 (Invitrogen) was utilized for plasmid/siRNA transfection and co-transfection according to the manufacturer's protocol.

Adenovirus infection

Recombinant adenovirus vectors for both overexpression and short hairpin RNA-mediated SIRT3 silencing were constructed and transfected as previously described. Cells in the logarithmic growth phase were seeded one day prior to transfection, with a cell density of approximately 50%. Subsequently, the culture media was replaced with serum-free DMEM medium, and the cells were infected with adenovirus at a multiplicity of infection (MOI) of 100:1.

Immunoprecipitation and immunoblot analysis

Cells were lysed and collected using RIPA lysis buffer (Beyotime, China) as previously outlined. The lysates were immunoprecipitated overnight at 4 °C with the appropriate antibodies, followed by the addition of protein A/G beads for 12 h. Subsequently, the immunoprecipitates underwent three washes, and an immunoblot analysis was conducted as previously described.

Statistical analysis

All statistical analyses were conducted using SPSS 20.0 statistical software. The data were presented as mean ± standard deviation, and a one-way analysis of variance (ANOVA) was employed to compare the different groups. In instances where ANOVA yielded significance, post hoc testing of group differences was carried out utilizing the least significant difference (LSD) test. A p-value < 0.05 was deemed to indicate statistical significance.

Results

SIRT3 ameliorates cognitive impairment in APP/PS1 mice

Mice were divided into four groups: wild-type mice as the control group (WT group), untreated APP/PS1 mice group (APP/PS1 group), APP/PS1 mice treated with adenoviral SIRT3 negative control group (APP/PS1 + SIRT3 NC group), and APP/PS1 mice treated with overexpressed adenoviral SIRT3 group (APP/PS1 + SIRT3 group). Preliminary evaluation of SIRT3 expression in each group revealed no difference in SIRT3 expression between the APP/PS1 group and the APP/PS1 + SIRT3 NC group; SIRT3 expression was significantly reduced in the APP/PS1 group compared with the WT group; and SIRT3 expression was significantly increased in the APP/PS1 group compared with the APP/PS1 + SIRT3 group (Fig. 1B–D). Subsequently, the Morris Water Maze (MWM) and Open Field Test (OFT) were performed on the WT group, APP/PS1 group, and APP/PS1 + SIRT3 NC group to assess the potential improvement of SIRT3 overexpression on cognitive deficits in APP/PS1 mice.

The OFT was performed first to assess the inherent anxiety-like state of the mice, given anxiety as a fundamental feature of AD. The results illustrated that the WT group displayed higher mobility and spent more time in the central area compared to the APP/PS1 + SIRT3 group, whereas the APP/PS1 + SIRT3

group exhibited increased mobility and spent more time in the central area compared to the APP/PS1 group (Fig. 2A–C). Subsequently, the MWM task was utilized to evaluate spatial learning and memory abilities. The results from the training phase indicated a noteworthy decrease in escape latency as the training progressed (Fig. 2D). During the probe trial, the APP/PS1 + SIRT3 group displayed a substantial increase in the percentage of time spent in the quadrant where the original platform was located and the frequency of crossing the platform (Fig. 2F, G). Although swimming speed and distance did not exhibit significant differences among the groups, the APP/PS1 + SIRT3 group swam a greater distance and at a higher speed compared to the APP/PS1 group (Fig. 2H, I). Overall, the behavioral experiments demonstrated that SIRT3 overexpression in APP/PS1 mice enhanced cognitive function and alleviated anxiety symptoms.

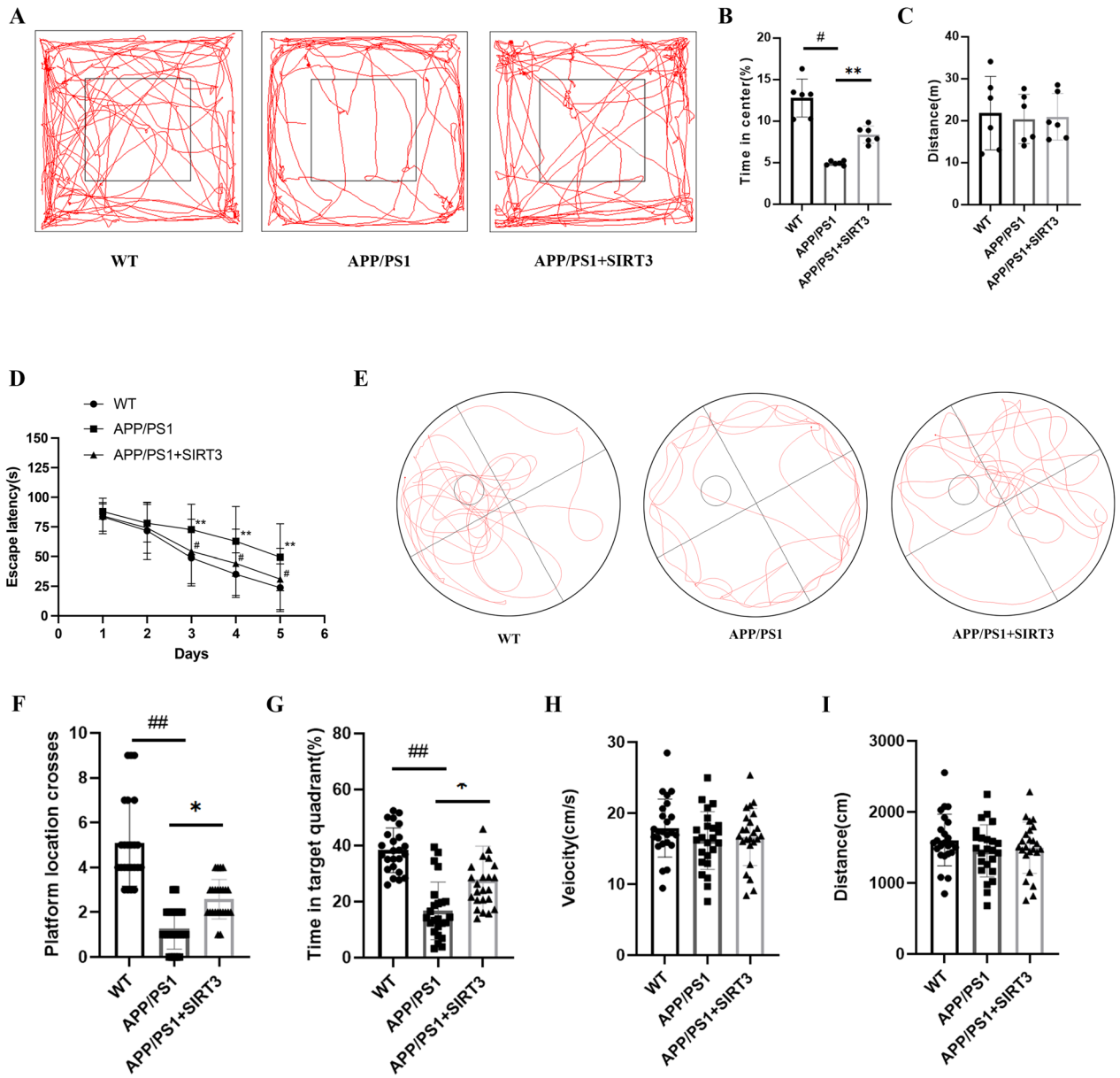

Fig. 2 SIRT3 mitigates cognitive impairment in APP/PS1 Mice. **A** Trajectory plots illustrating mice movement during the open field test, **B** proportion of time spent in the central region, **C** distance traveled. Throughout the initial 5 days of spatial exploration in the water maze experiments, **D** latency for mice to reach the platform; on the 6th day of spatial exploration, **E** trajectory plots of mice movement, **F** frequency of platform crossings by the mice, **G** percentage of time spent in the platform quadrant, **H** velocity and **I** distance. n = 6; $^{**}P < 0.01$; $^{\#}P < 0.05$

To enhance the reliability of the experiment, we added a control group (without behavioral experiments) and an intervention group (water maze and open field tests) to detect the expression of SIRT3, CHAT, and GFAP proteins, aiming to evaluate the impact of behavioral training on molecules. The results showed that behavioral training alone did not significantly affect the expression of these proteins. The new data reinforced the conclusion that the observed molecular changes were more likely directly related to our intervention measures (see Fig. 1 in Supplementary Information 2).

SIRT3 promotes hippocampal neurogenesis in APP/PS1 mice

Following the completion of MWM and OFT assessments, our subsequent investigation aimed to determine the potential of SIRT3 in enhancing cognitive function by promoting hippocampal neurogenesis. Comprehensive evaluations of morphology and pathological alterations in the CA1, CA3, and DG regions of the hippocampal tissue were conducted using HE and Nissl staining techniques. The results from HE staining revealed that, compared to the WT group, the neuronal nuclei in the APP/PS1 group displayed shrinkage and irregular morphology, along with a reduced number of pyramidal cells in the hippocampus, indicating pathological changes in the APP/PS1 group. Importantly, the upregulation of SIRT3 effectively prevented neuronal loss in the hippocampal region (Fig. 3C, F), suggesting a supportive role of SIRT3 in promoting hippocampal neurogenesis in APP/PS1 mice. Similarly, Nissl staining identified neuronal impairment in the hippocampal CA1, CA3, and DG regions. The hippocampal tissue of mice in the WT group exhibited an abundance of Nissl bodies in the cytoplasm and normal nucleoli. In contrast, the hippocampus of APP/PS1 mice showed significant reductions in Nissl bodies and nucleoli, indicative of neuronal damage. Notably, intervention with SIRT3 resulted in varying degrees of restoration in the neuronal status of the mice hippocampus (Fig. 3D, G).

Furthermore, double-cortin (DCX) immunofluorescence staining was employed to identify immature neurons. Our observations revealed a significant reduction in the number of DCX-positive (DCX+) cells within the hippocampus of APP/PS1 mice compared to their WT counterparts. Interestingly, the overexpression of SIRT3 in the cohort of APP/PS1 mice resulted in a restoration of the number of DCX + cells in the hippocampal region (Fig. 3E, H). These findings provide compelling evidence supporting the significant enhancement of hippocampal neurogenesis in APP/PS1 mice facilitated by SIRT3.

Overexpression of SIRT3 attenuates the deposition of Aβ in the *hippocampus* of APP/PS1 mice

To investigate the impact of SIRT3 on amyloid plaque burdens, immunofluorescence staining for Aβ plaques was conducted on brain tissue sections. The results revealed a significant decrease in the numbers of Aβ deposition and the total area of plaques in the CA1, CA3, and DG regions of the hippocampus in the APP/PS1 + SIRT3 group compared to the APP/PS1 group (Fig. 4B, C). This indicates that SIRT3 may alleviate Aβ deposition.

SIRT3 regulates the activation of neural stem cells and the activation of the Wnt/β-catenin pathway

We proved SIRT3-mediated NSC proliferation through EdU experiments (Fig. 5), and the results showed that the EdU level was significantly increased after overexpression of SIRT3, while it was decreased after knockdown of SIRT3.

To elucidate the underlying mechanisms of SIRT3-mediated NSC differentiation, we investigated the protein expression of ChAT and GFAP in NSCs under RA induction (10 μM), along with the protein expression of β-catenin, DVL, GSK-3α, and GSK-3β within the Wnt/β-catenin pathway. Our findings reveal that upon SIRT3 overexpression, there was a significant decrease in the levels of GFAP, phosphorylated β-catenin (p-β-catenin; Ser33/37/Thr41), GSK3α, and GSK3β, whereas the levels of ChAT, DVL, β-catenin, phosphorylated GSK3α (p-GSK3α; Ser21), and phosphorylated GSK3β (p-GSK3β; Ser9) were markedly elevated (Fig. 5). Conversely, SIRT3 knockout in C17.2 cells produced opposite effects. These results suggest that SIRT3-induced NSC differentiation may be contingent upon the activation of the Wnt/β-catenin pathway.

Subsequently, we delved into the investigation of how SIRT3 modulates NSC proliferation and RA-induced

(See figure on next page.)

Fig. 3 SIRT3 mitigates neuronal impairment in APP/PS1 mice. **A**–**B** Schematic diagram of the CA1, CA3, and DG regions of the hippocampus in mice. **C** HE staining of neurons in CA1, CA3 and DG regions of mice hippocampus. **D** Nissl staining of the CA1, CA3, and DG regions in the mice hippocampus. **E** Representative areas displaying DCX-positive cells in the dentate gyrus of the hippocampus. The red rectangles outline the CA1, CA3, and DG regions. Scale bar: 500 μm. Quantitative assessment of HE staining (**F**) and Nissl bodies (**G**) in the hippocampal CA1, CA3, and DG regions. **H** Quantification of DCX-positive cells (green) in each group. n = 6; *P < 0.05, **P < 0.01, ***P < 0.005 and ****P < 0.001; $^{\#}$P < 0.05, $^{\#\#}$P < 0.01 and $^{\#\#\#}$P < 0.005. *WT* wild-type, *DG* dentate gyrus, *SD* standard deviation

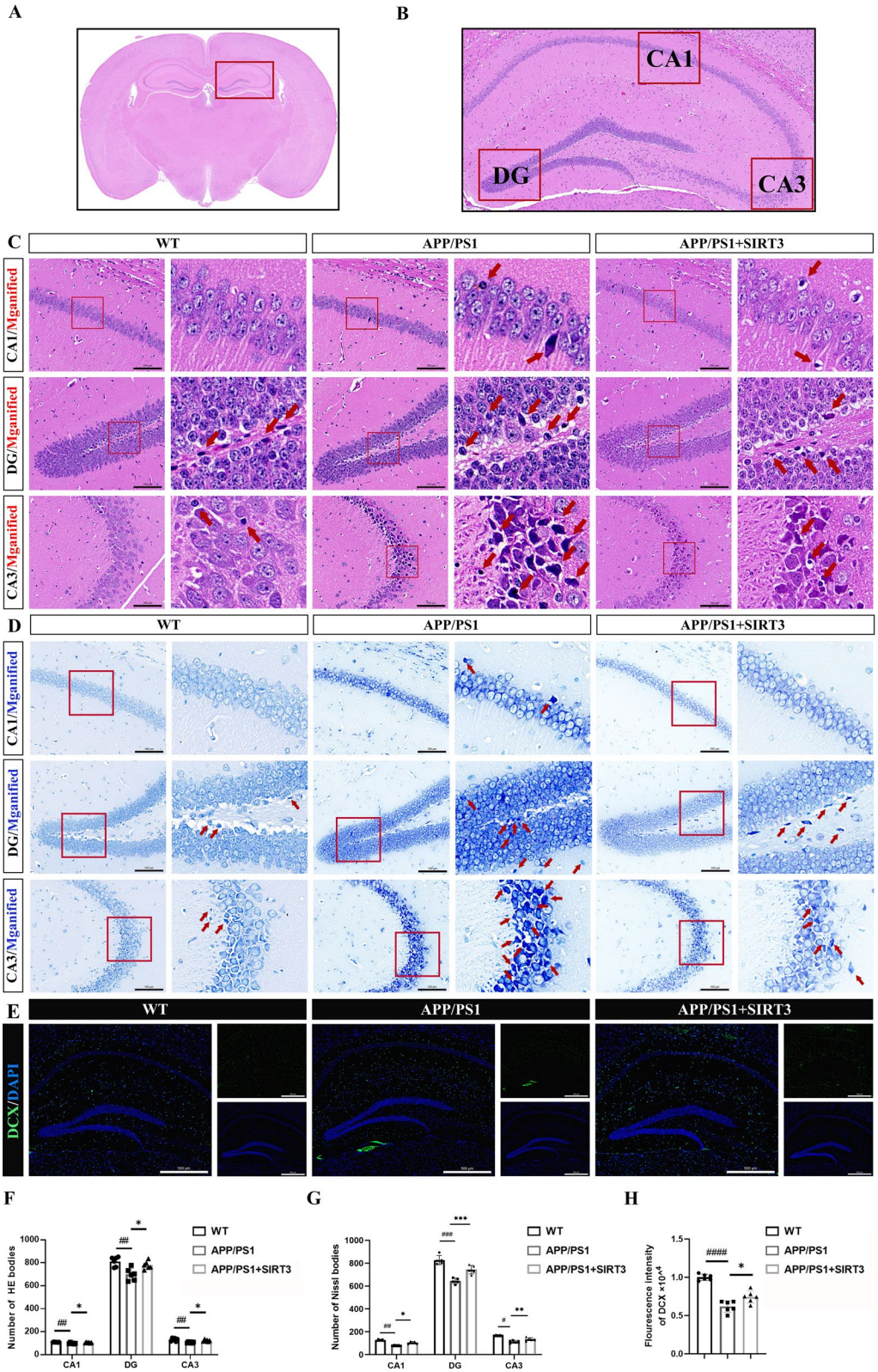

Fig. 3 (See legend on previous page.)

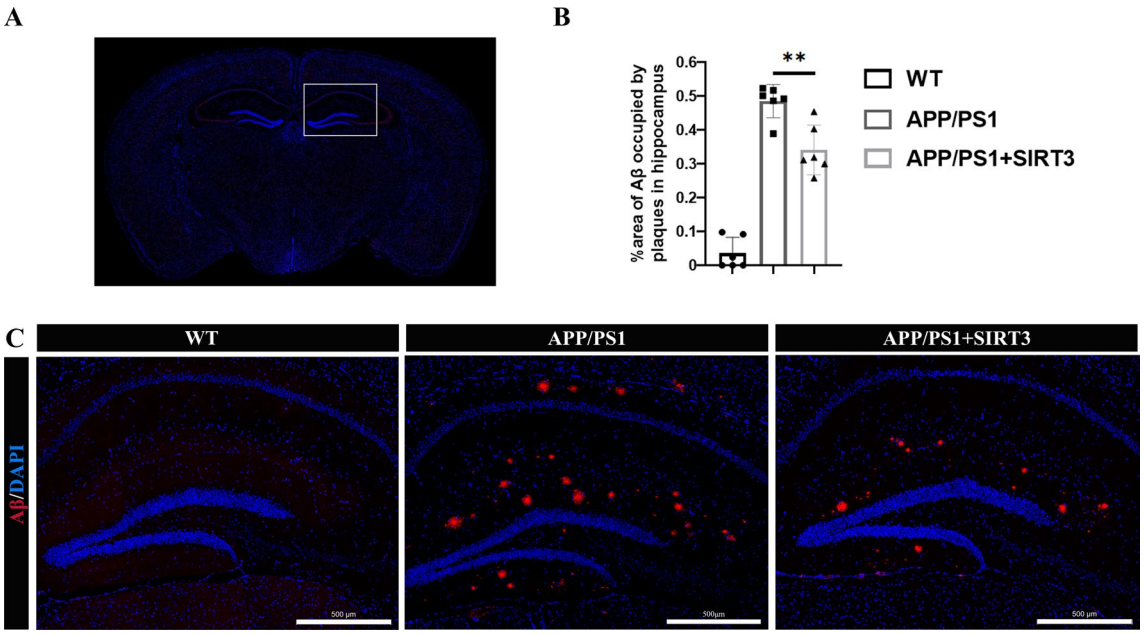

Fig. 4 SIRT3 alleviates hippocampal Aβ accumulation in APP/PS1 mice. **A** Schematic diagram of the hippocampus in mice. **C** Visualization of Aβ (red) deposition in the hippocampus. Scale bar: 500 μm. **B** Quantitative analysis of Aβ deposition in each experimental group. n = 6; $^{\#\#}P < 0.01$. *WT* wild-type; *DG* dentate gyrus, *SD* standard deviation

NSC differentiation through factors within the Wnt/β-catenin pathway.

GSK3α and GSK3β negatively regulates the proliferation of NSCs in co-culture model

Quantitative analysis of hippocampal cell counts in vivo, performed through HE staining and Nissl staining, demonstrated that SIRT3 promotes cellular proliferation in the hippocampal region (Fig. 3A–D, F, G). In vitro, Edu assays revealed that SIRT3 enhances the proliferation of NSCs and inhibits the expression of GSK3 isoenzymes within the Wnt/β-catenin pathway in NSCs induced by RA. To investigate whether GSK3 isoenzymes impact NSC proliferation independently, this study utilized co-culture models to explore the roles of GSK3α and GSK3β in NSC proliferation. Plasmid-mediated overexpression and siRNA-mediated gene knockdown were employed to manipulate the expression of GSK3α/β in C17.2 cells, with the effectiveness of transduction validated by WB and RT-PCR (Fig. 6A–F). Subsequent CCK-8 and EdU assays indicated that overexpression of GSK3α/β significantly diminished NSC proliferation, whereas knockdown of GSK3α/β promoted NSC proliferation. Notably, GSK3α played a more prominent role than GSK3β in regulating NSC proliferation (Fig. 7C–E). In summary, these findings suggest that GSK3α/β exerts inhibitory effects on NSC proliferation in co-culture models, with GSK3α being the primary contributor to this process. This study provides valuable insights into the distinct functions of GSK3α and GSK3β in NSC proliferation, uncovering their potential as therapeutic targets for modulating NSC proliferation.

SIRT3 modulates neural stem cell differentiation through regulation of the GSK3β/β-catenin pathway

WB analysis revealed that SIRT3 inhibits the expression of GSK3 isoenzymes within the Wnt/β-catenin pathway in NSCs induced by RA (Fig. 5). Subsequently, the study on the effect of GSK3α/β on NSC differentiation induced by RA was conducted by detecting three neuronal markers (Nestin, Tuj1, and GFAP) (Fig. 8A–D). Immunocytochemical staining showed that the presence of GSK3α/β reduced Tuj1-positive cells and increased Nestin-positive cells, while having no significant impact on GFAP-positive cells. Conversely, siRNA-mediated knockdown of GSK3α/β significantly increased the differentiation of NSCs into neurons (Tuj1- and Nestin-positive cells) while decreasing GFAP-positive cells. WB results indicated that overexpression of GSK3α/β led to reduced Tuj1 expression with no notable change in GFAP levels, whereas knockdown had the opposite effect. Notably, GSK3β exhibited a more pronounced influence on NSC differentiation compared to GSK3α.

Further research was conducted to explore whether SIRT3 regulates NSC differentiation by inhibiting

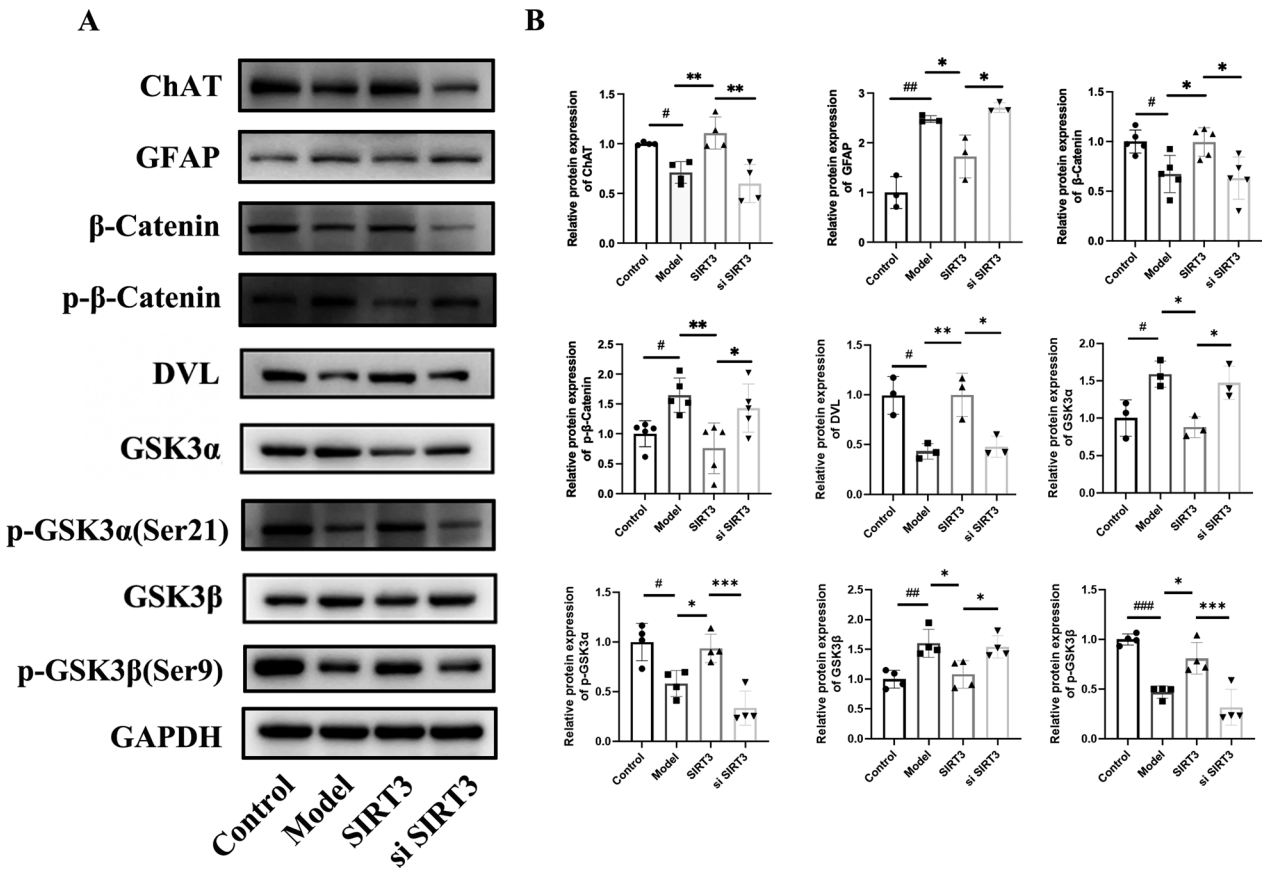

Fig. 5 SIRT3 regulates the activation of the Wnt/β-catenin pathway. Representative Western blot bands (**A**) and densitometric quantifications (**B**) for ChAT, GFAP, DVL, GSK3α, p-GSK3α (Ser 21), GSK3β, p-GSK3β (Ser 9), β-Catenin, and p-β-Catenin. $^{\#}P < 0.05$, $^{\#\#}P < 0.01$, $^{\#\#\#}P < 0.005$; $^{*}P < 0.05$, $^{**}P < 0.01$, $^{***}P < 0.005$. Full-length blots are provided in Supplementary Fig. 1

GSK3β and subsequently suppressing downstream β-Catenin expression.

The results demonstrated (Figs. 5A–B and 8E-F) that overexpression of SIRT3 promoted neuronal differentiation of NSCs and expression of p-GSK3β(ser6), p-β-Catenin, and ChAT, while inhibiting astrocytic differentiation and expression of GSK3β, p-β-Catenin, and GFAP. The reverse was observed upon SIRT3 downregulation. WB analysis (Fig. 8E, F) showed that when a GSK3β inhibitor (CHIR-99021) was used in combination with SIRT3 knockdown, β-Catenin expression was significantly reduced compared to CHIR-99021 treatment alone. Although no significant difference was observed in p-β-Catenin expression, there was a trend towards increased levels in the si SIRT3/CHIR-99021 group compared to the CHIR-99021 group alone. Based on these findings, we hypothesize that under RA induction, SIRT3 may promote NSC differentiation towards neurons by inhibiting GSK3β expression, thereby enhancing downstream β-Catenin expression.

Cholinergic neurogenesis is associated with GSK3 downregulation

In the context of AD, it is widely acknowledged that the loss of basal forebrain cholinergic neurons contributes to deficits in memory and attention. ISL1, a pivotal homeobox transcription factor, holds a crucial role in regulating the ontogeny of cholinergic neurons. To further elucidate the function of GSK3α/β in cholinergic neurogenesis, we utilized immunofluorescence and Western blot techniques to assess the protein levels of ISL1 and ChAT (Fig. 9). Western blot analysis revealed that the si GSK3α/β group exhibited significantly higher ISL1 protein levels compared to the model group. Conversely, in NSCs overexpressing GSK3α/β, ISL1 expression was markedly reduced. Immunofluorescence staining corroborated these findings, with the si GSK3α/β group displaying an increased number of ISL1-positive cells, predominantly due to GSK3β downregulation, and the inverse pattern observed in the overexpression group. These results are in line with our previous findings in

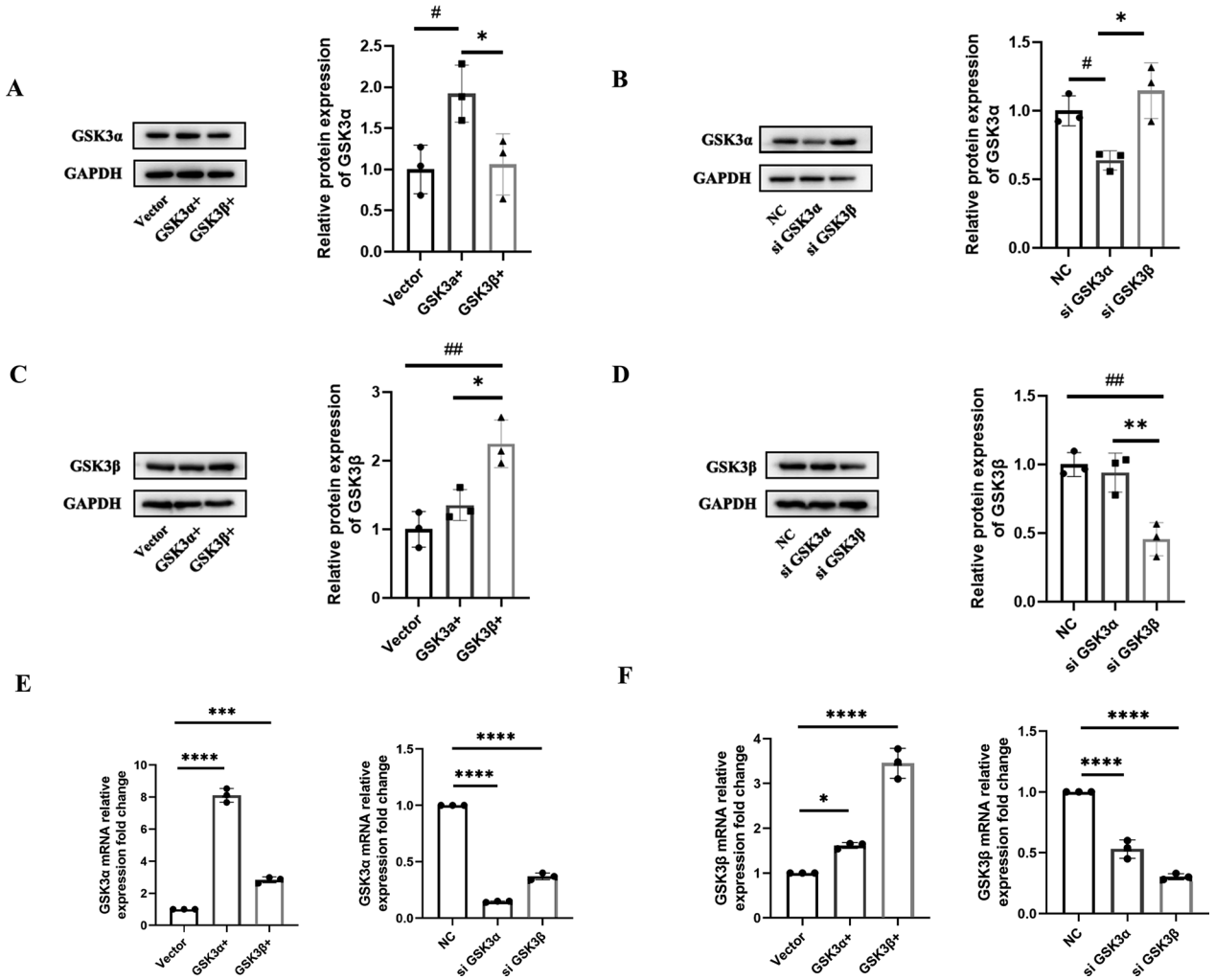

Fig. 6 Overexpression and knockdown of GSK3α/β were confirmed by immunoblot analysis and RT-PCR analysis in NSCs. Overexpression (**A**) and knockdown (**B**) of GSK3α protein were confirmed by western blot analysis. Overexpression (**C**) and knockdown (**D**) of GSK3β protein were confirmed by western blot analysis. Overexpression and knockdown of GSK3α (**E**) or GSK3β (**F**) mRNA were confirmed by qPCR. *P < 0.05, **P < 0.01, ****P < 0.001, ns: no significant difference P > 0.05. Full-length blots are presented in Supplementary Fig. 1

section"GSK3α and GSK3β negatively regulates the proliferation of NSCs in co-culture model", indicating that intervening in the SIRT3/GSK3/ISL1 pathway appears to be a promising strategy for enhancing cholinergic neurogenesis.

SIRT3-DVLs interactions in regulating NSC apoptosis within a co-culture model

The study confirmed that SIRT3 inhibits NSC apoptosis induced by microglia activation, with concurrent upregulation of DVLs protein expression. Analysis using Annexin V-FITC/PI staining revealed that co-transfection of DVL siRNA and SIRT3 overexpression adenovirus increased NSC apoptosis, while co-transfection of SIRT3 shRNA and DVL plasmid reduced apoptosis compared to SIRT3 shRNA alone, indicating DVL's role in mitigating NSC apoptosis resulting from SIRT3 knockdown (Fig. 10A, B). Furthermore, investigations showed that SIRT3 overexpression increased mRNA and protein levels of DVL, while SIRT3 inhibition led to decreased DVL expression (Fig. 10C–F). Co-immunoprecipitation assays demonstrated a direct interaction between DVL1/2/3 and SIRT3 in HEK293T cells, as well as a potential interaction between SIRT3 and DVL2/3 in C17.2 cells, highlighting the mechanistic role of SIRT3-DVL collaboration in regulating NSC apoptosis (Fig. 10G, H).

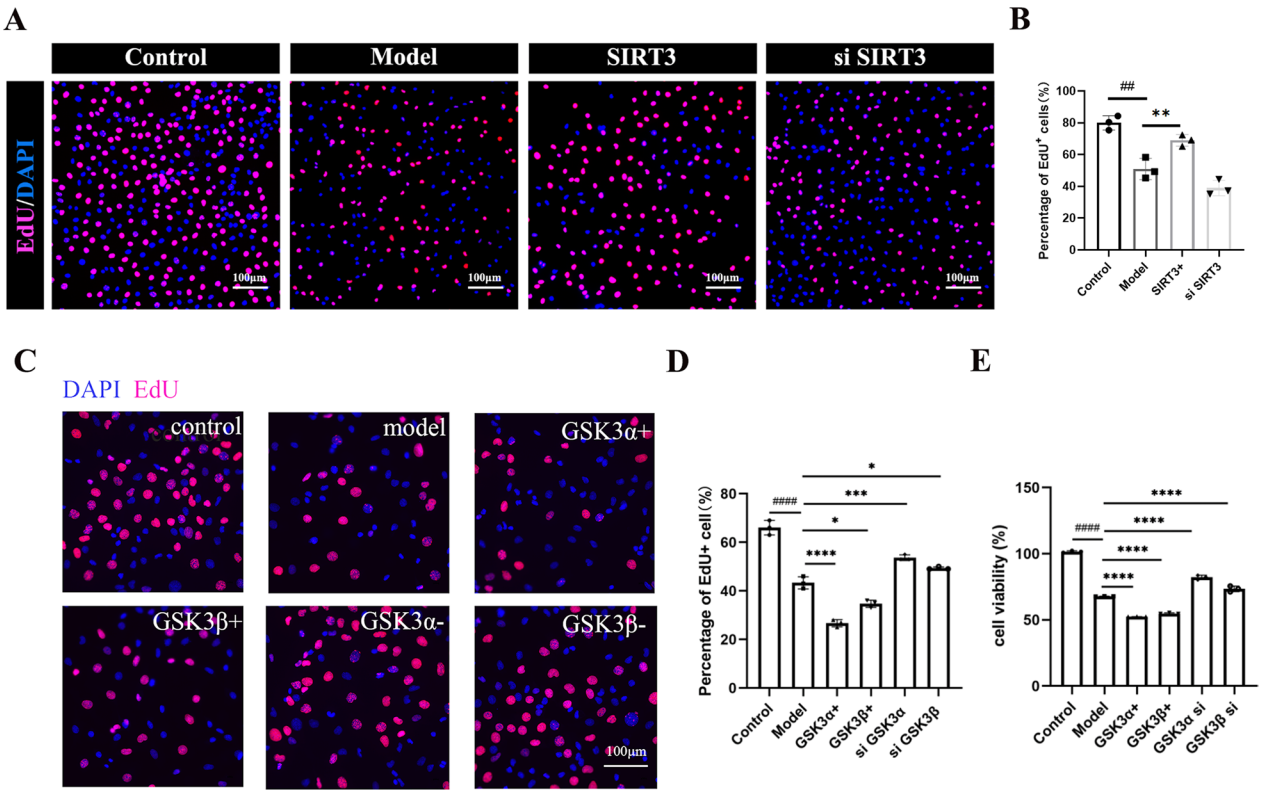

Fig. 7 SIRT3 regulates the proliferation of neural stem cells. EdU fluorescence images (**A**) and quantitative graphs (**B**) showing SIRT3 promoting proliferation in C17.2 cells. Scale bar: 100 μm. **C** and **D** Representative images and quantitative statistics of EdU-positive cells in each group. Scale bar: 100 μm. **E** The effect of GSK3α/β overexpression or siRNA on NSC proliferation was evaluated by CCK-8 assay. n = 3; $^{\#\#}P < 0.01$and $^{\#\#\#\#}P < 0.0001$; $^{*}P < 0.05$, $^{**}P < 0.01$, $^{***}P < 0.005$ and $^{****}P < 0.001$. Data are mean ± SEM

Discussion

Alzheimer's disease (AD) is characterized by progressive memory loss and overall cognitive decline. However, current Aβ-targeting methods can only slow down the progression of AD but cannot reverse or even stop the disease process. The rescue of cells or cell therapy in both early and late stages of AD is crucial for improving patients' quality of life. Therefore, we will focus our research attention on improving cell function and how to prevent or even reverse cognitive decline [26, 27]. Our study has elucidated the role and potential mechanisms of SIRT3 in NSCs neurogenesis and its impact on learning and cognitive functions in APP/PS1 mice. The results demonstrated that cognitive deficits were significantly mitigated by SIRT3, accompanied by a reduction in hippocampal Aβ deposition and enhanced neurogenesis in the hippocampal region of APP/PS1 mice. Concurrently, SIRT3 facilitated neurogenesis through the activation of the DVL/GSK3/ISL1 signaling pathway. Within this pathway, GSK3α plays a crucial role in NSCs proliferation, GSK3β predominantly influences NSCs differentiation, and DVLs mitigate the increase in NSCs apoptosis triggered by Aβ-mediated microglia activation. These findings suggest that SIRT3 may confer potential neuroprotective effects via the DVL/GSK3/ISL1 pathway.

Studies have uncovered the intricate role of the sirtuins family, particularly SIRT3, in promoting neurogenesis and reducing Aβ deposition [28]. The sirtuins family utilizes NAD + as a substrate to facilitate the binding and deacetylation of proteins involved in DNA damage repair, inflammation regulation, and antioxidant defense mechanisms [29]. SIRT3's neuroprotective effects are evident in its ability to promote neurogenesis, as demonstrated in a recent study showing SIRT1's significant role in enhancing the differentiation potential of NSCs [30]. Our current findings indicate that SIRT3 not only boosts neurogenesis but also reduces Aβ deposition, consistent with previous research showing SIRT3's ability to mitigate cellular damage caused by microglia activation in NSCs. However, the underlying mechanism of SIRT3's neurogenic effects remains largely unexplored. The mechanisms involved in SIRT3's reduction of Aβ deposition in the hippocampus are multifaceted. SIRT3 can promote autophagy to reduce neuronal damage, enhance microglia's recognition and removal of Aβ, and regulate energy metabolism, mitochondrial function, and oxidative stress

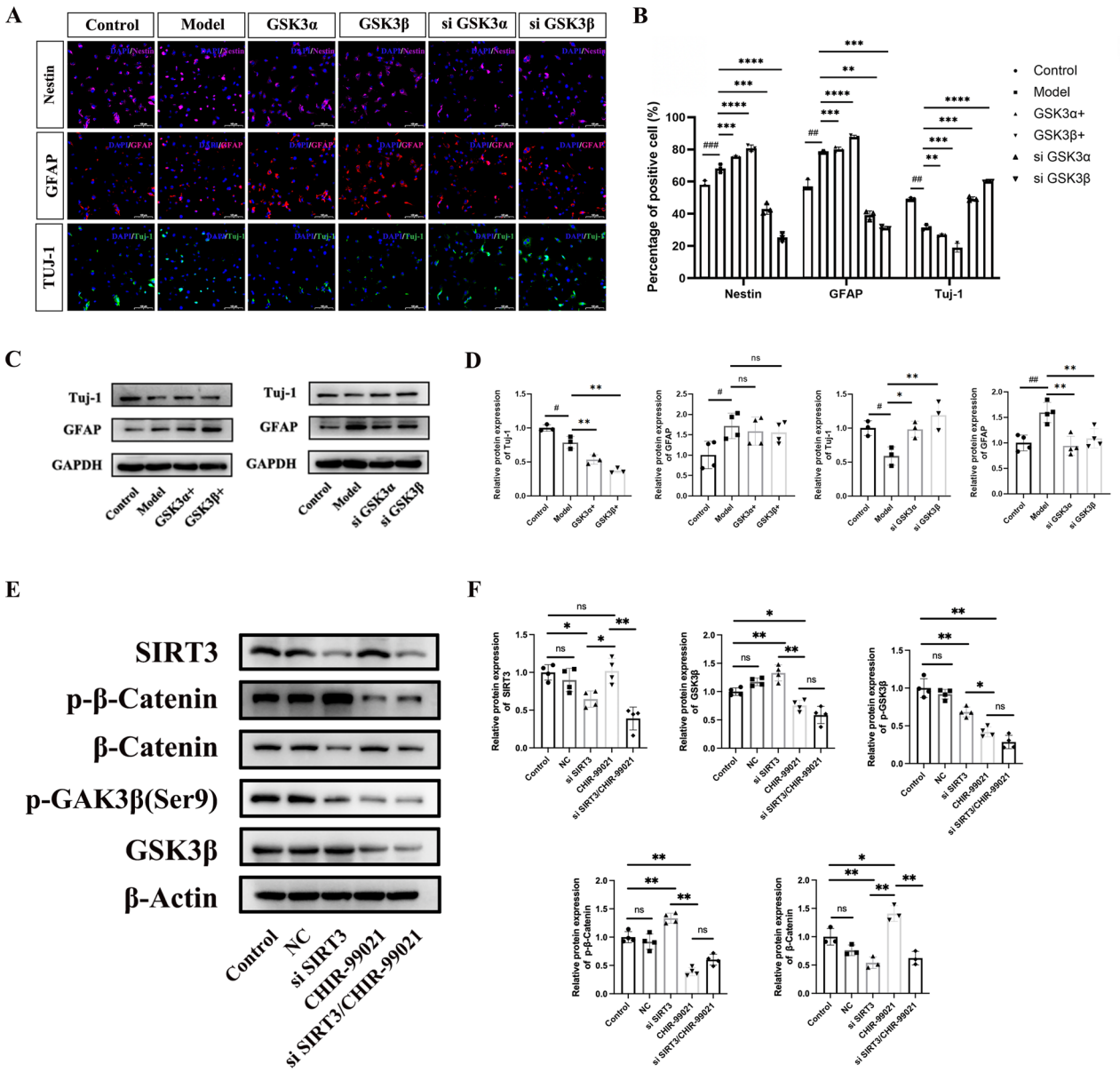

Fig. 8 GSK3α/β inhibited the proliferation and differentiation of NSCs in co-culture model. Immunofluorescence (**A**) and quantification of percentage of active cells (**B**) for GFAP (red) and Tuj-1 (green). representative protein blot bands (**C**) and densitometric quantification (**D**) for GFAP and Tuj-1. Representative Western blot bands (**E**) and densitometric quantifications (**F**) for SIRT3, p-β-Catenin, β-Catenin, p-GSK3β (Ser 9) and GSK3β. n = 3; $^{\#}P < 0.05$, $^{\#\#}P < 0.01$ and $^{\#\#\#}P < 0.001$; $^{*}P < 0.05$, $^{**}P < 0.01$, $^{***}P < 0.005$ and $^{****}P < 0.001$; ns: no significance. Data are mean ± SEM. Full-length blots are presented in Supplementary Fig. 1

processes, thereby reducing Aβ production and promoting its clearance. SIRT3 may also influence Aβ metabolism through other signaling pathways or molecules. These mechanisms are anticipated to safeguard neurons and decelerate the progression of neurodegenerative diseases.

Through our research, we have discovered that SIRT3 can significantly improve neurogenesis in AD by regulating the WNT/β-catenin pathway. The WNT/β-catenin pathway plays a pivotal role in the neurogenesis mechanism of AD, regulating the proliferation and differentiation of NSCs and affecting neuronal survival, synaptic function, and neural network remodeling. By activating this pathway, β-catenin accumulates in the cytoplasm and enters the nucleus, activating downstream transcription factors, which promote the differentiation of NSCs into neurons [31]. This process is particularly crucial in AD models, as the loss of neurons and the degeneration

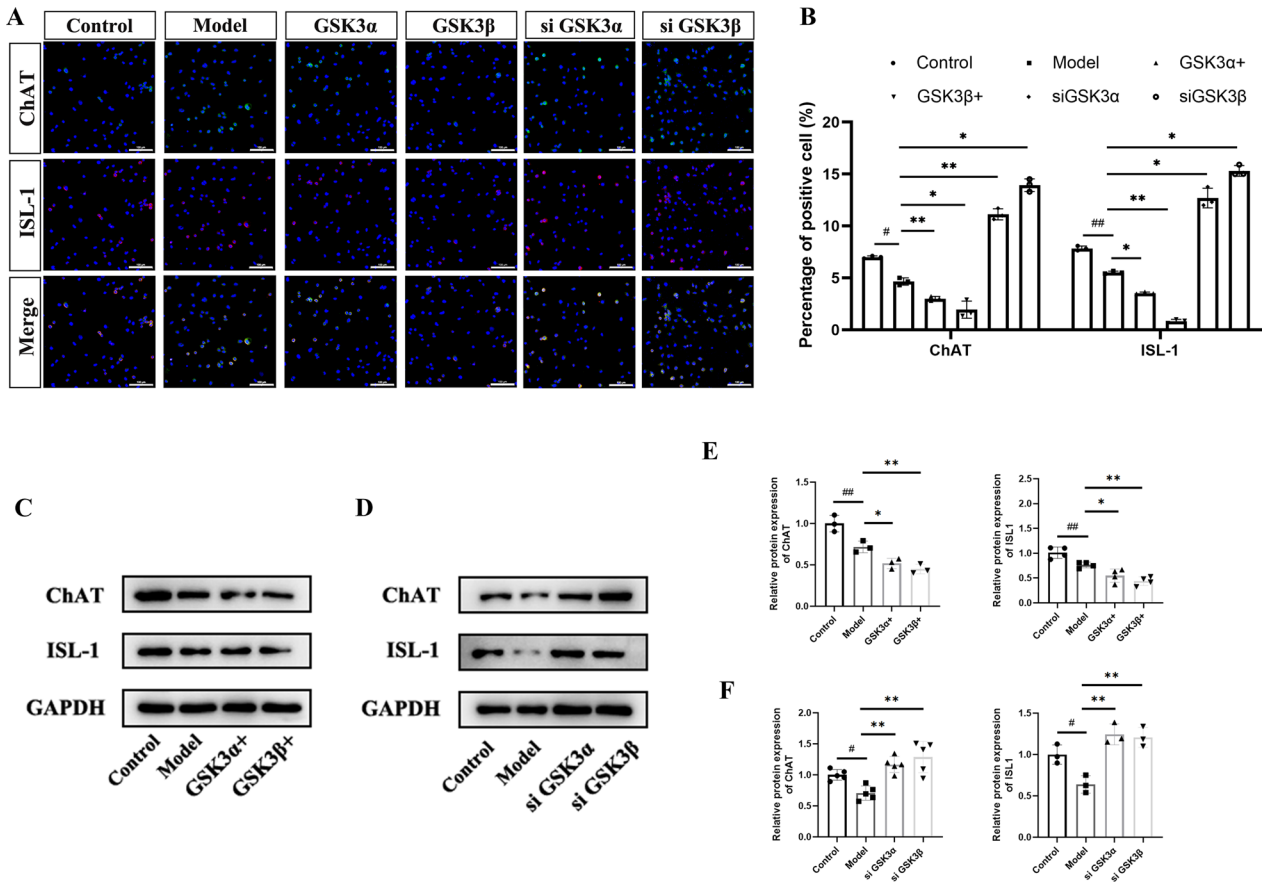

Fig. 9 GSK3 downregulation promotes differentiation of NSCs to cholinergic neurons. Immunofluorescence images of ChAT (green) and ISL-1 (red) positive cells in each group (**A**) and statistical plots of the percentage of positive cells (**B**). **C**–**F** Western blot detected the expression of ChAT and ISL-1 in differentiating NSCs. n = 3; $^{\#}P < 0.05$, $^{\#\#}P < 0.01$; $^{*}P < 0.05$, $^{**}P < 0.01$. Full-length blots are presented in Supplementary Fig. 1

of neural functions are the main causes of cognitive decline in AD patients. The activation of the WNT/β-catenin pathway can not only increase the number of neurons, but also regulate synaptic plasticity and maintain the integrity of the blood–brain barrier [32, 33]. Moreover, it participates in the learning and memory mechanisms through the normal phosphorylation of tau, while alleviating the production and aggregation of Aβ caused by WNT/β-catenin dysfunction. In addition, the WNT/β-catenin pathway can also regulate neurogenesis processes through interactions with other signaling pathways, making WNT/β-catenin signaling disorders of certain importance in AD-related research [31–34]. However, the specific roles of the various factors in the WNT/β-catenin pathway remain to be further explored.

Neurogenesis, the process by which NSCs proliferate and differentiate to generate new functional neurons, is essential for the proper development and functional connectivity of the mammalian brain [35, 36]. The microenvironment plays a crucial role in influencing neurogenesis [37, 38]. Recent work by Lu has highlighted the significant impact of the aberrant AD microenvironment on microglial behavior, thereby hastening the progression of AD [39]. In our previous study, we demonstrated that Aβ-induced activation of microglia can directly trigger oxidative stress injury and elevate the rate of cell apoptosis, a phenomenon that can be mitigated by SIRT3 [14]. Moreover, SIRT3 has been shown to alleviate cognitive impairment by suppressing hippocampal neuroinflammation [40]. More recently, SIRT3 has been found to safeguard GABAergic neurons from degeneration induced by Aβ [41].

The LIM homeodomain transcription factor ISL-1 is expressed in multiple organs and plays a crucial role during embryonic development. ISL-1 coordinates the generation of cholinergic neurons in the spinal cord and forebrain, making it a promising candidate for determining the fate of different types of cholinergic cells in the central nervous system [42]. During early development, ISL-1 is expressed in both cholinergic and non-cholinergic striatal neurons. As differentiation progresses, ISL-1 expression becomes restricted to cholinergic neurons

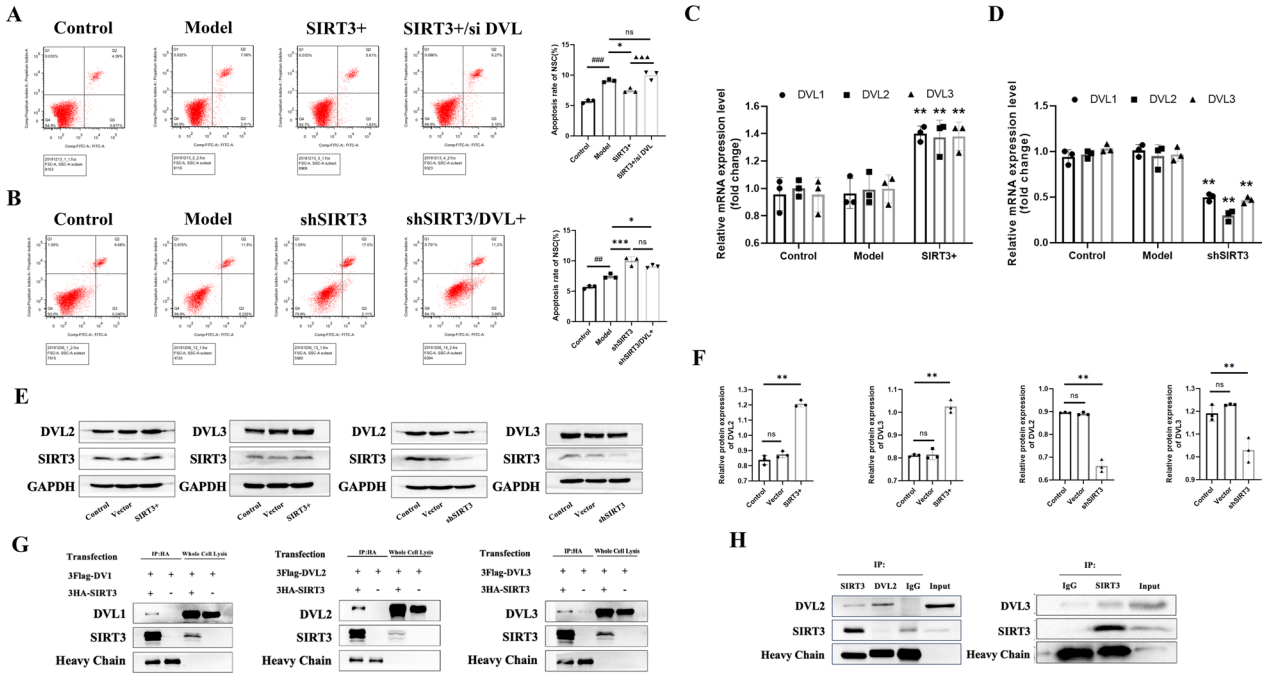

Fig. 10 SIRT3 interacts with DVLs and The Effects of SIRT3 and DVLs on apoptosis of NSCs. **A** The effects of SIRT3 overexpression and DVLs interference on apoptosis of NSCs. **B** Effects of SIRT3 overexpression and DVLs interference on apoptosis of NSC induced by Aβ-mediated microglia activation. Effects of SIRT3 overexpression and SIRT3 interference on DVL2 and DVL3 mRNA expression levels (**C** and **D**) and protein expression levels (**E** and **F**) **G** immunoprecipitation of FLAG-tagged DVL1/2/3 co-precipitates HA-tagged SIRT3 from HEK293T cells expressing both tagged proteins. **H** Interaction between endogenous SIRT3 and DVL2/3 by Immunoprecipitation-Western bloting. n = 3; *P < 0.05, **P < 0.01, ***P < 0.005; $^{\#}$P < 0.01, $^{\#\#}$P < 0.01, $^{\#\#\#}$P < 0.005; ▲▲▲P < 0.005; ns: no significance. Full-length blots are presented in Supplementary Fig. 1

and is suppressed in non-cholinergic neurons [43]. This study investigated the regulatory role of GSK3 on neuronal subtype-specific markers ChAT and ISL-1 proteins. The results indicate that GSK3 negatively regulates the expression of ChAT and ISL-1 proteins. Inhibition of GSK3 was found to promote differentiation of neural stem cells into cholinergic neurons in co-culture systems, suggesting a potential therapeutic effect on memory impairments. Building upon these findings, our data suggest that SIRT3 exerts a neuroprotective effect by promoting neurogenesis.

GSK3, highly expressed in the brain and spinal cord, is implicated in the pathogenesis of AD [44–46]. Glycogen synthase kinase 3 (GSK-3) comprises two isoforms, GSK3α and GSK3β, each with similar yet distinct roles [47–49]. Variations in the expression of GSK3α and GSK3β have been observed in prostate tumors, with GSK3β exerting a more significant influence than GSK3α on androgen receptor transcriptional activity reduction [47]. Furthermore, inhibition of GSK3β, but not GSK3α, has been shown to reduce Aβ deposition and neuritic plaque formation [50]. Notably, the majority of studies have focused on GSK3β rather than GSK3α. In our investigation, we compared the effects of GSK3α and GSK3β on NSCs proliferation and differentiation. Our findings revealed that GSK3α plays a more pivotal role than GSK3β in NSCs proliferation, whereas GSK3β predominates in NSCs differentiation. Thus, our study indicates that the two GSK3 isoforms play distinct roles in regulating NSCs behavior.

SIRT1 has been identified as a key regulator of Wnt signaling. Deletion of SIRT1 has been shown to decrease the protein levels of all three DVLs and enhance Wnt-stimulated cell migration. Moreover, immunoprecipitation experiments have revealed the in vivo complex formation between SIRT1 and DVLs [51]. This discovery directly establishes a connection between Sirtuins and DVLs, shedding light on the multiple physiological responses mediated by SIRT1. Saxena et al. demonstrated the essential role of SIRT1 activity in modulating DVL1 and TIAM1 levels in cancer cells [52]. In our investigation, we unveiled, for the first time, a direct association between SIRT3 and DVLs, providing further insights into the interplay between the Sirtuin family and the Wnt signaling pathway. Furthermore, SIRT3 demonstrates protective and anti-apoptotic effects on NSCs, likely through its interaction with DVLs and the regulation of its expression. Nevertheless, our study faces several limitations. Our smaller sample size may constrain the broader applicability of our findings. The western blotting

experiments targeting DVL1 could not be completed due to the unavailability of specific antibodies in the market. Future research is warranted to validate the interaction between SIRT3 and DVLs, as well as to explore the precise structural domains involved in the binding between SIRT3 and DVLs.

To summarize, the current understanding of SIRT3's influence on neurogenesis in NSCs remains limited, and the potential link to the Wnt/β-catenin pathway's regulation remains elusive. In this study, we propose a novel hypothesis wherein SIRT3 promotes neurogenesis via the Wnt/β-catenin pathway, thereby safeguarding NSCs from microglial activation-induced damage. Leveraging an NSC-microglia transwell co-culture model, we intend to elucidate the functional role and underlying mechanism of SIRT3 in neurogenesis. Our anticipated findings will not only establish SIRT3 as a positive regulator of neural differentiation, accompanied by Wnt/β-catenin signaling activation, but also provide novel insights into the distinct roles of GSK3α and GSK3β in NSC proliferation and differentiation. Moreover, SIRT3's capacity to mitigate NSC apoptosis in the context of microglial activation, primarily through its interaction with DVLs, offers promising implications for the development of innovative therapeutic strategies for NSC-related disorders.

Conclusion

To the best of our knowledge, this represents the inaugural report delineating the involvement of the Wnt/β-catenin signaling pathway in SIRT3-mediated neuroprotection. Our study demonstrates that SIRT3 prompts NSCs differentiation, with an accompanying activation of the Wnt/β-catenin signaling pathway during this process. Mechanistically, we have discerned distinct roles for the two isoforms of GSK3 in NSCs proliferation and differentiation. Furthermore, we have illustrated that SIRT3 confers protective and anti-apoptotic effects on NSCs, potentially through its binding to DVLs and regulation of their expression. These findings unveil a novel mechanism of neurogenesis, thereby offering potential insights into therapeutic strategies for neurodegenerative diseases such as AD.

Supplementary Information

The online version contains supplementary material available at https://doi.org/10.1186/s13287-024-03925-8.

Additional file 1.

Additional file 2.

Acknowledgments
Not applicable.

Author contributions
YW was involved in the coordination and design of the study. ND performed most of the animal experiments, XS and AL performed most of the cell culture experiments, and ND and XS performed the statistical analysis of the results and drafted the manuscript. JL and DJ performed some of the cell culture experiments, drew the illustrations, and critically revised the manuscript. All authors agree that all issues related to the accuracy or completeness of the paper were properly investigated and resolved, and final approval was given for the version to be published. All authors read and approved the final manuscript.

Funding
This study was supported by the Natural Science Foundation of Guangdong Province, 2020A1515010230 , Guangdong Yiyang Healthcare Charity Foundation, JZ2022010 and National Natural Science Foundation of China 82474102.

Availability of data and materials
The datasets utilized in this study can be obtained from the corresponding author upon reasonable request. This paper does not report original code. Any additional information required to reanalyze the data reported in this paper is available from the lead contact upon request.

Declarations

Ethics approval and consent to participate
All animal studies were conducted in accordance with the ARRIVE guidelines and approved by the Ethics Committee of Pearl River Hospital of Southern Medical University (Mechanisms of Improving Postoperative Cognitive Remission after APP/PS1 Mouse Stem Cell Therapy by Sal; Ethics Committee of Pearl River Hospital of Southern Medical University Approval Document; Approval Reference No. LAEC-2024-013; Date, January 30, 2024).

Consent for publication
Not applicable.

Competing interests
All authors declare no potential conflict of interest.

Author details
[1]Department of Pharmacy, Zhujiang Hospital, Southern Medical University, Guangzhou 510282, Guangdong, China. [2]Department of Pharmacy, Women and Children's Hospital, School of Medicine, Xiamen University, 10# Zhenhai Road, Xiamen, China. [3]Department of Pharmacy, Shenzhen Second People's Hospital, Shenzhen 518000, China. [4]Department of Biology and Pharmacy, Yulin Normal University, Yulin 537000, Guangxi, China. [5]Laboratory of Research of New Chinese Medicine, Zhujiang Hospital, Southern Medical University, Guangzhou 510282, Guangdong, China.

Received: 22 March 2024 Accepted: 4 September 2024
Published online: 12 September 2024

References

1. Long JM, Holtzman DM. Alzheimer disease: an update on pathobiology and treatment strategies. Cell. 2019;179(2):312–39.
2. Yoo S, Blackshaw S. Regulation and function of neurogenesis in the adult mammalian hypothalamus. Prog Neurobiol. 2018;170:53–66.
3. Whitehouse PJ, Price DL, Struble RG, et al. Alzheimer's disease and senile dementia: loss of neurons in the basal forebrain. Science. 1982;215(4537):1237–9.
4. Mehta D, Jackson R, Paul G, et al. Why do trials for Alzheimer's disease drugs keep failing? A discontinued drug perspective for 2010–2015. Expert Opin Investig Drugs. 2017;26(6):735–9.
5. Cummings J, Aisen PS, Dubois B, et al. Drug development in Alzheimer's disease: the path to 2025. Alzheimer's Res Therapy. 2016;8:39.
6. Cope EC, Gould E. Adult neurogenesis, glia, and the extracellular matrix. Cell Stem Cell. 2019;24(5):690–705.

7. Haigis MC, Deng CX, Finley LW, et al. SIRT3 is a mitochondrial tumor suppressor: a scientific tale that connects aberrant cellular ROS, the Warburg effect, and carcinogenesis. Can Res. 2012;72(10):2468–72.
8. He J, Shangguan X, Zhou W, et al. Glucose limitation activates AMPK coupled SENP1-Sirt3 signalling in mitochondria for T cell memory development. Nat Commun. 2021;12(1):4371.
9. Van de Ven RAH, Santos D, Haigis MC. Mitochondrial sirtuins and molecular mechanisms of aging. Trends Mol Med. 2017;23(4):320–31.
10. McDonnell E, Peterson BS, Bomze HM, et al. SIRT3 regulates progression and development of diseases of aging. Trends Endocrinol Metab. 2015;26(9):486–92.
11. Han P, Tang Z, Yin J, et al. Pituitary adenylate cyclase-activating polypeptide protects against β-amyloid toxicity. Neurobiol Aging. 2014;35(9):2064–71.
12. Lee J, Kim Y, Liu T, et al. SIRT3 deregulation is linked to mitochondrial dysfunction in Alzheimer's disease. Aging cell. 2018;17(1):66.
13. Santos SS, Moreira JB, Costa M, et al. The mitochondrial antioxidant Sirtuin3 cooperates with lipid metabolism to safeguard neurogenesis in aging and depression. Cells. 2021;11(1):66.
14. Jiang DQ, Wang Y, Li MX, et al. SIRT3 in neural stem cells attenuates microglia activation-induced oxidative stress injury through mitochondrial pathway. Front Cell Neurosci. 2017;11:7.
15. Tsuchida T, Ensini M, Morton SB, et al. Topographic organization of embryonic motor neurons defined by expression of LIM homeobox genes. Cell. 1994;79(6):957–70.
16. Elshatory Y, Gan L. The LIM-homeobox gene Islet-1 is required for the development of restricted forebrain cholinergic neurons. J Neurosci. 2008;28(13):3291–7.
17. Marchetti B, Tirolo C, L'Episcopo F, et al. Parkinson's disease, aging and adult neurogenesis: Wnt/β-catenin signalling as the key to unlock the mystery of endogenous brain repair. Aging Cell. 2020;19(3): e13101.
18. da Silva F, Zhang K, Pinson A, et al. Mitotic WNT signalling orchestrates neurogenesis in the developing neocortex. EMBO J. 2021;40(19): e108041.
19. Heppt J, Wittmann MT, Schäffner I, et al. β-catenin signaling modulates the tempo of dendritic growth of adult-born hippocampal neurons. EMBO J. 2020;39(21):e104472.
20. Telias M, Ben-Yosef D. Pharmacological manipulation of Wnt/β-Catenin signaling pathway in human neural precursor cells alters their differentiation potential and neuronal yield. Front Mol Neurosci. 2021;14: 680018.
21. Schneider R, Koop B, Schröter F, et al. Activation of Wnt signaling promotes hippocampal neurogenesis in experimental autoimmune encephalomyelitis. Mol Neurodegener. 2016;11(1):53.
22. Sun X, Peng X, Cao Y, et al. ADNP promotes neural differentiation by modulating Wnt/β-catenin signaling. Nat Commun. 2020;11(1):2984.
23. Marchetti B. Wnt/β-Catenin signaling pathway governs a full program for dopaminergic neuron survival, neurorescue and regeneration in the MPTP mouse model of Parkinson's disease. Int J Mol Sci. 2018;19(12):66.
24. Silverman DA, Martinez VK, Dougherty PM, et al. Cancer-associated neurogenesis and nerve-cancer cross-talk. Can Res. 2021;81(6):1431–40.
25. Mazemondet O, Hubner R, Frahm J, et al. Quantitative and kinetic profile of Wnt/β-catenin signaling components during human neural progenitor cell differentiation. Cell Mol Biol Lett. 2011;16(4):515–38.
26. Taguchi A, Okinaka Y, Takeda A, Okamoto T, Boltze J, Claussen C, Gul S. Activation of neurogenesis in the hippocampus is a novel therapeutic target for Alzheimer's disease. Neuroprotection. 2023;1(2):139–42.
27. Liu J, van Beusekom H, Bu XL, Chen G, Rosado Henrique, de Castro P, Chen X, Chen X, Clarkson AN, Farr TD, Fu Y, Jia J, Jolkkonen J, Kim WS, Korhonen P, Li S, Liang Y, Liu GH, Liu G, Liu YH, Malm T, Mao X, Oliveira JM, Modo MM, Ramos-Cabrer P, Ruscher K, Song W, Wang J, Wang X, Wang Y, Wu H, Xiong L, Yang Y, Ye K, Yu JT, Zhou XF, Zille M, Masters CL, Walczak P, Boltze J, Ji X, Wang YJ. Preserving cognitive function in patients with Alzheimer's disease: The Alzheimer's disease neuroprotection research initiative (ADNRI). Neuroprotection. 2023;1(2):84–98.
28. Culig L, Chu X, Bohr VA. Neurogenesis in aging and age-related neurodegenerative diseases. Ageing Res Rev. 2022;78: 101636.
29. Dai H, Sinclair DA, Ellis JL, et al. Sirtuin activators and inhibitors: promises, achievements, and challenges. Pharmacol Ther. 2018;188:140–54.
30. Fan W, Tang S, Fan X, et al. SIRT1 regulates sphingolipid metabolism and neural differentiation of mouse embryonic stem cells through c-Myc-SMPDL3B. eLife. 2021;10:66.
31. Yu M, Qin K, Fan J, Zhao G, Zhao P, Zeng W, Chen C, Wang A, Wang Y, Zhong J, Zhu Y, Wagstaff W, Haydon RC, Luu HH, Ho S, Lee MJ, Strelzow J, Reid RR, He TC. The evolving roles of Wnt signaling in stem cell proliferation and differentiation, the development of human diseases, and therapeutic opportunities. Genes Dis. 2023;11(3): 101026.
32. Fessel J. The several ways to authentically cure Alzheimer's dementia. Ageing Res Rev. 2023;92: 102093.
33. Wang Q, Huang X, Su Y, Yin G, Wang S, Yu B, Li H, Qi J, Chen H, Zeng W, Zhang K, Verkhratsky A, Niu J, Yi C. Activation of Wnt/β-catenin pathway mitigates blood–brain barrier dysfunction in Alzheimer's disease. Brain. 2022;145(12):4474–88.
34. Jia L, Piña-Crespo J, Li Y. Restoring Wnt/β-catenin signaling is a promising therapeutic strategy for Alzheimer's disease. Mol Brain. 2019;12(1):104. https://doi.org/10.1186/s13041-019-0525-5.
35. Ming GL, Song H. Adult neurogenesis in the mammalian brain: significant answers and significant questions. Neuron. 2011;70(4):687–702.
36. Zhao C, Deng W, Gage FH. Mechanisms and functional implications of adult neurogenesis. Cell. 2008;132(4):645–60.
37. Couch ACM, Berger T, Hanger B, et al. Maternal immune activation primes deficiencies in adult hippocampal neurogenesis. Brain Behav Immun. 2021;97:410–22.
38. Büttner R, Schulz A, Reuter M, et al. Inflammaging impairs peripheral nerve maintenance and regeneration. Aging Cell. 2018;17(6):e12833.
39. Lu Y, Guo Z, Zhang Y, et al. Microenvironment remodeling micelles for Alzheimer's disease therapy by early modulation of activated microglia. Adv Sci. 2019;6(4):1801586.
40. Liu Q, Sun YM, Huang H, et al. Sirtuin 3 protects against anesthesia/surgery-induced cognitive decline in aged mice by suppressing hippocampal neuroinflammation. J Neuroinflammation. 2021;18(1):41.
41. Cheng A, Wang J, Ghena N, et al. SIRT3 Haploinsufficiency aggravates loss of GABAergic interneurons and neuronal network hyperexcitability in an Alzheimer's disease model. J Neurosci. 2020;40(3):694–709.
42. Ericson J, Thor S, Edlund T, et al. Early stages of motor neuron differentiation revealed by expression of homeobox gene Islet-1. Science. 1992;256(5063):1555–60.
43. Pfaff SL, Mendelsohn M, Stewart CL, et al. Requirement for LIM homeobox gene Isl1 in motor neuron generation reveals a motor neuron-dependent step in interneuron differentiation. Cell. 1996;84(2):309–20.
44. Sayas CL, Ávila J. GSK-3 and Tau: A key duet in Alzheimer's disease. Cells. 2021;10(4):66.
45. Hur EM, Zhou FQ. GSK3 signalling in neural development. Nat Rev Neurosci. 2010;11(8):539–51.
46. Zhang S, Lachance BB, Mattson MP, et al. Glucose metabolic crosstalk and regulation in brain function and diseases. Prog Neurobiol. 2021;204: 102089.
47. Darrington RS, Campa VM, Walker MM, et al. Distinct expression and activity of GSK-3α and GSK-3β in prostate cancer. Int J Cancer. 2012;131(6):E872–83.
48. Doble BW, Patel S, Wood GA, et al. Functional redundancy of GSK-3alpha and GSK-3beta in Wnt/beta-catenin signaling shown by using an allelic series of embryonic stem cell lines. Dev Cell. 2007;12(6):957–71.
49. Mishra R, Nagini S, Rana A. Expression and inactivation of glycogen synthase kinase 3 alpha/beta and their association with the expression of cyclin D1 and p53 in oral squamous cell carcinoma progression. Mol Cancer. 2015;14:20.
50. Ly PT, Wu Y, Zou H, et al. Inhibition of GSK3β-mediated BACE1 expression reduces Alzheimer-associated phenotypes. J Clin Investig. 2013;123(1):224–35.
51. Holloway KR, Calhoun TN, Saxena M, et al. SIRT1 regulates Dishevelled proteins and promotes transient and constitutive Wnt signaling. Proc Natl Acad Sci USA. 2010;107(20):9216–21.
52. Saxena M, Dykes SS, Malyarchuk S, et al. The sirtuins promote Dishevelled-1 scaffolding of TIAM1, Rac activation and cell migration. Oncogene. 2015;34(2):188–98.

Publisher's Note